MR Image reconstruction from under-sampled measurements using local and global sparse representations

Mengran Lin, Yongxin Ge, Mingjian Hong*

Chongqing University, Shapingba District, Chongqing, China

Abstract—we proposed a novel imaging model combining both local and global sparsity constraints to capture details and overall structures of MR images. Firstly, the local sparse representations are obtained via dictionary leaning followed by sparse coding upon learned dictionary which are trained from specific image. Secondly, traditional analytical dictionaries are used to promote global sparsity of the MR image. Finally, the reconstruction is solved using a nonlinear conjugate gradient with known local and global sparsity constraints. This procedure is repeated iteratively to improve the quality of reconstruction. The performance of the proposed method is evaluated using a brain data set. Experimental results demonstrate a better image quality with an improvement of 1~6dB for reduction factor up to 10 comparing to the existing state-of-the-art method.

***Index Terms*—Compressed sensing (CS), dictionary leaning, local and global sparsity, magnetic resonance imaging (MRI).**

I. INTRODUCTION

Magnetic resonance imaging (MRI) has become a powerful noninvasive diagnostic imaging technique since its invention. However, MRI is a relatively slow imaging modality due to the physical or physiological constraints [1]. To speed up the imaging process, a number of measurements required for reconstruction are reduced without degrading the image quality. Compressive sensing (CS) [2-4], which can faithfully recover signals from under-sampled measurements, fits the problem of MRI and has become very popular in recent years. CS requires the image being recovered has a sparse representation in some dictionaries, which can be categorized in two ways.

The first one, namely global sparse dictionary, can yield a sparse representation for a whole image, such as wavelets [5], curvelets [6], singular value decomposition (SVD) [7] among others. However, these global dictionaries lose some fine features of the image such as edges, as shown in Fig. 1b, which is reconstructed by CS-MRI [5] using wavelet(db4) as the global sparsifying dictionary.

The second one, namely local sparse dictionary learned from specific image patches, can sparsify all patches of the image, such as K-SVD [8-10], which is used in DLMRI (dictionary learning MRI) [13] to reconstruct MR image from under-sampled k-space measurements. Specifically, the local dictionary based methods represent an image as an array of patches, and then seeks a sparse representation of the image by learning an local sparse dictionary [12, 13]. However, these methods ignore the information of an image as a whole when promoting the local sparsity, and lead to loss of global structure information of the image as shown in Fig. 1c, which is reconstructed by DLMRI with non-overlapping patch size 10x10.

In this work, we proposed a novel imaging model named GLSMRI (Global and Local Sparsity-constrained MRI), representing the sparse structure of the MR image by exploiting both the local and global sparse dictionaries, to reconstruct the image faithfully [5] from under-sampled measurements. The proposed model consists of two sub-models: 1) a local sparse model attempts to encode all patches of the image sparsely by learning an over-complete patch-level dictionary. 2) a global sparse model represents the whole image sparsely using a predefined sparse dictionary. Compared to DLMRI, which use least squares to reconstruct image and may suffer from the over-fitting, GLSMRI prevent over-fitting by adding L1 regularization in the second sub-model. Our model can be solved within traditional CS framework [15] and can refine the solution iteratively. GLSMRI is then evaluated by using a brain data set [20]. Several important parameters of the GLSMRI are evaluated and discussed.

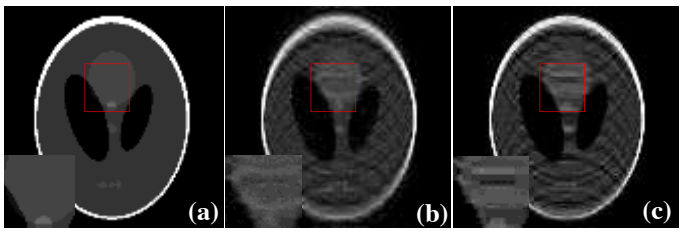

Fig. 1. Comparison of images reconstructed from 10 fold under-sampled k-space data exploiting global and local sparsity. (a) is the ground truth, (b) is the result of CS-MRI using wavelet(db4) as the global sparsifying transform, (c) is the result of DLMRI with non-overlapping patch size 10x10.

II. PROPOSED METHOD

A. *Imaging model*

Existing methods reconstruct the image using only the global or local sparse structure of the image and exhibit some aforementioned shortcomings. We propose GLSMRI to

reconstruct the image by combining both global and local sparse representation of image as follows:

$$\boldsymbol{P_0}: \min_{X,D,\Lambda} \|\mathrm{Y} - F_u\mathrm{X}\|_2^2 + \lambda_\mathrm{L} \sum_{\mathrm{ij}} \left\|R_{ij}X - D\alpha_{ij}\right\|_2^2 + \lambda_G \|\psi X\|_1 \quad \text{s.t. } \left\|\alpha_{ij}\right\|_0 \le T_0 \ \forall\, i,j \tag{1}$$

where, X is the image to be reconstructed, Y is the under-sampled k-space measurement, and F_u is the partial Fourier transform. The term $\|\mathrm{Y} - F_u\mathrm{X}\|_2^2$ in $\boldsymbol{P_0}$ holds data consistency in k-space. In the second term of $\boldsymbol{P_0}$, namely $\lambda_\mathrm{L} \sum_{\mathrm{ij}} \left\|R_{ij}X - D\alpha_{ij}\right\|_2^2$, R_{ij} is patch extraction operation, and D is the learned dictionary under which the corresponding patch $R_{ij}X$ has sparse representation α_{ij} constrained by sparse level T_0 and $\Lambda = \{\alpha_{ij} | \forall\, i,j\}$. In the last term $\lambda_G \|\psi X\|_1$ of $\boldsymbol{P_0}$, sparse representation of X is obtained directly under ψ which is the global sparse dictionary depicted in introduction. The parameters λ_L and λ_G are used to promote and balance the local or global sparsity. Obviously, when $\lambda_\mathrm{L} = 0$ or $\lambda_\mathrm{G} = 0$, the model degrades to the DLMRI or CS-MRI, respectively.

B. The algorithm of Imaging model

Problem $\boldsymbol{P_0}$ is solved using two alternated procedures. First, the dictionary D is learned from an initial guess of the image, and then sparse representation α_{ij} of each image patch is obtained. Second, image X is reconstructed under the CS framework with both local and global sparsity constraints. These two steps are further detailed in the following subsections.

1) Dictionary learning

In this step, K-SVD is used to train a dictionary D from fixed X by solving the following sub-problem:

$$\boldsymbol{P_1}: \min_{D,\Lambda} \sum_{\mathrm{ij}} \left\|R_{ij}X - D\alpha_{ij}\right\|_2^2 \quad \text{s.t. } \left\|\alpha_{ij}\right\|_0 \le T_0 \ \forall\, i,j \tag{2}$$

once D is learnt, α_{ij} is determined by sparse coding X on D solved by OMP [16] and [17]. In our implementation, only a fraction of image patches of X are randomly chosen when training D. After D and α_{ij} are obtained, we have a coarse estimation X^* of target image as following if patches at image boundaries are wrapped around [13].

$$X^* = \frac{\sum_{ij} R_{ij}^T D^* \alpha_{ij}^*}{c} \tag{3}$$

c is the number of patches contributing to a pixel and can be calculated using $c = n/r^2$, where n is number of pixels of a patch and r is the overlap stride, which measures the distance between two adjacent patches. X^* will be the start point of the second procedure.

2) Reconstruction

GLSMRI formulates the reconstruction with known D^* and α_{ij}^* as follows:

$$\mathbf{p_2}: \min_{\mathrm{X}} f(X) = \|\mathrm{Y} - F_u\mathrm{X}\|_2^2 + \lambda_L \sum_{\mathrm{ij}} \left\|R_{ij}X - D^*\alpha_{ij}^*\right\|_2^2 + \lambda_G \|\psi X\|_1 \tag{4}$$

Sub-problem $\boldsymbol{P_2}$ falls into the CS framework and can be solved using non-linear conjugate gradient method [18]. The gradient corresponding to $\boldsymbol{P_2}$ is:

$$\nabla f(X) = 2\lambda_L \sum_{\mathrm{ij}} (\mathrm{R}_{\mathrm{ij}}^T R_{ij}X - \mathrm{R}_{\mathrm{ij}}^T D^* \alpha_{ij}^*) + 2F_u^\mathrm{H}(F_u\mathrm{X} - \mathrm{Y}) + \lambda_G \nabla(\|\psi X\|_1) \tag{5}$$

which can be reduced to [5, 13]

$$\nabla f(X) = 2\lambda_L \beta(X - X^*) + 2F_u^\mathrm{H}(F_u\mathrm{X} - \mathrm{Y}) + \lambda_G \nabla(\|\psi X\|_1) \tag{6}$$

These two steps can be iterated to improve the output of previous iteration, as shown in Fig. 2.

Compared to the DLMRI, GLSMRI has two improvements:

(a) DLMRI solves the equation $2\lambda_L\beta(X - X^*) + 2F_u^\mathrm{H}(F_u\mathrm{X} - \mathrm{Y}) = 0$ using least squares technique. Because the X^* is just a coarse estimation, the solution of least squares usually over-fits the X^* and inherits the blocky effects from X^*. While the GLSMRI enforces L1 regularization to prevent over-fitting and to refine the solution iteratively from X^* within CS framework.

(b) The least squares solution of DLMRI equals to k-space back-filling, which fills the frequencies of non-sampled pixels using that of X^* and restores the frequencies of sampled pixels by weighted averaging the frequencies of X^* and sampled values. However, the sampled values will overwhelm the frequencies of X^* assuming little noise when measuring. While the GLSMRI solves Eq. (5) implicitly uses nonlinear conjugate gradient solver, which is more versatile and can append additional regularization terms to enforce other structural constraints, to improve X^*.

To verify the arguments, we compared GLSMRI with CS-MRI and DLMRI in the same condition as the Fig. 1 and the results are shown in Fig. 3, which shows that DLMRI introduces the blocky effect when reconstructing, while GLSMRI suppresses the blocky effect by balancing the weights for local and global sparsity.

III. EXPERIMENTS AND RESULTS

The GLSMRI was evaluated using axial brain with size of 512x512, which was obtained from [20].

Two sampling patterns, Cartesian random sampling along the phase-encoding direction (Fig. 4a) and 2D random sampling (Fig. 4b), were used in the following evaluations. They used 1D and 2D Gaussian distributions respectively, which had denser sampling at the center of k-space [5].

The code of K-SVD was taken from [13], and non-linear conjugate gradient solver [18] was modified from CS-MRI [5] to fit our model. All simulations and reconstructions were implemented in MATLAB R2012b (MathWorks, Natick, MA).

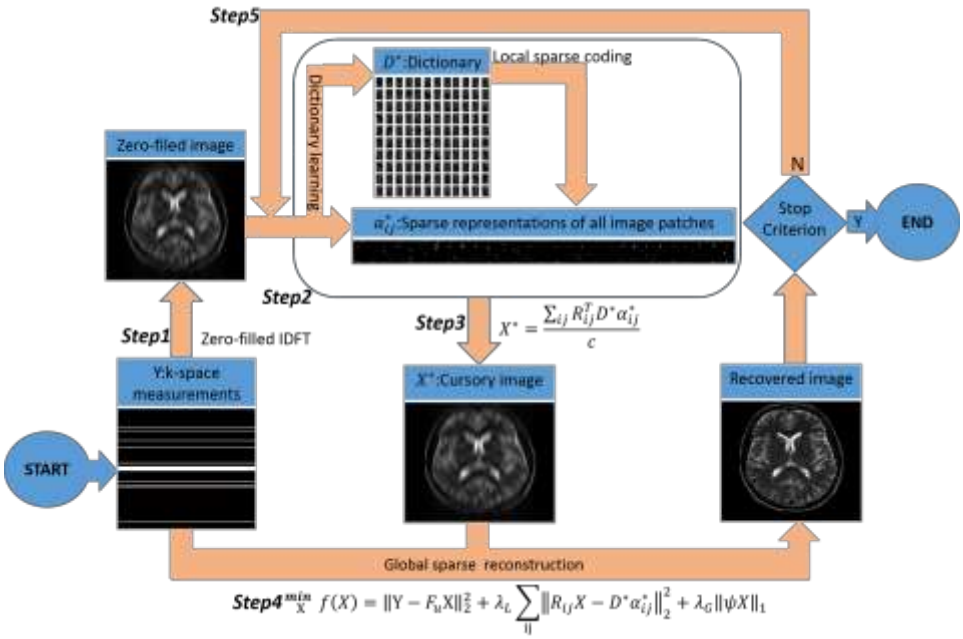

Fig. 2. Flowchart of the GLMRI reconstruction model.

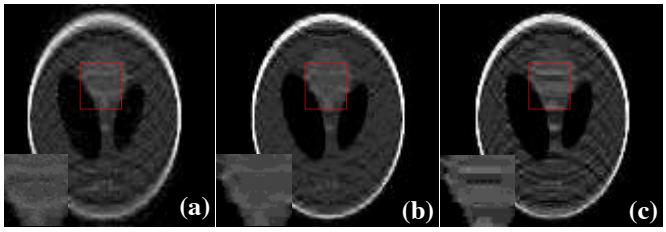

Fig. 3. Comparison of images reconstructed by CS-MRI (a) using wavelet (db4) as global sparsifying dictionary, GLSMRI (b) and DLMRI (c) with non-overlapping patch size 10x10. The reduction factor is 10.

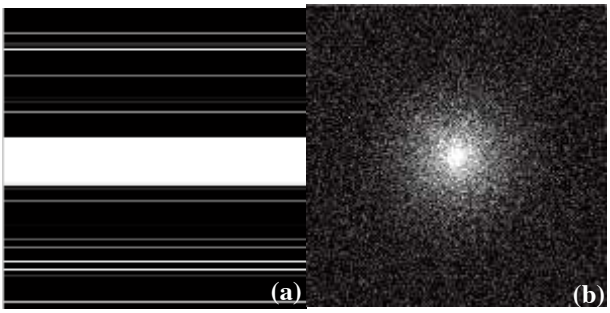

Fig. 4. Cartesian (a) and 2D (b) random sampling patterns.

Several parameters of the model were fixed in the evaluations and discussed later on. The patch size was set to 6x6, dictionary size to 36, overlap stride to 1, the number of patches for training to 5000. We used the Daubechies wavelet db4 as the global sparse dictionary ψ [5] . The quality of the recovered image was quantified using peak signal-to-noise ratio (PSNR) [19]. The GLSMRI was compared with DLMRI to show improved performance and how the global sparsity constraint affected the recovered images. For this dataset, we set $\lambda_L = 50$ and $\lambda_G = 1/300$, which meant the local sparsity was weighted 50 times more than the global sparsity.

In Fig. 5, although no visual difference could be seen in recovered brain images as shown in Fig. 5(b)-(c), GLSMRI outperformed DLMRI as shown in the Fig. 5(g), especially in the peaks and valleys marked by arrows. The error maps in Figs. 5(e)-(f) reveal that GLSMRI recovers more details of the image than that of DLMRI. And this held true for various reduction factors as shown in Fig. 5(h). When 2D random sampling pattern was used as shown in Fig. 6, the difference between two methods was enlarged. The GLSMRI followed the ground truth well as shown in Fig. 6g, especially at the positions near peak and valley. The output of GLSMRI was stable after 6 iterations, while DLMRI got stable until 11 iterations as shown in Fig. 5(d) and Fig. 6(d). In the end, GLSMRI got 1.8dB larger in PSNR than DLMRI. The error map of DLMRI contained notable structure information while that of GLSMRI contained almost the random noise as demonstrated in Fig. 6(e)-(f).

We evaluated several important parameters of GLSMRI by varying one of them at a time while keeping the rests fixed to find an optimal combination of parameters. The brain data was used for evaluation under 2D random sampling at the reduction factor 4. For the overlap stride r, Fig. 7a shows that the PSNR decreases gradually with the increasing of r, so the best choice is $r = 1$. To select best combination of λ_L and λ_G, λ_L was firstly fixed to $1/300$. PSNR versus the ratio λ_L/λ_G of weights for local and global sparsities, which balanced the local and global sparsities, as shown in Fig. 7b. It show that PSNR gets larger with the increasing of λ_L/λ_G from 0, in which case GLSMRI is equivalent to CS-MRI, and is stable for $\lambda_L/\lambda_G \geq 40$, then PSNR turns lower gradually as λ_L/λ_G tends to be infinity, in which case the GLSMRI degrades to the DLMRI.

As a result, $\lambda_L/\lambda_G = 50$ is a reasonable choice. Finally, with fixed $\lambda_L/\lambda_G = 50$ the trend of PSNR versus λ_L suggests $\lambda_L = 1/300$ is appropriate as shown in Fig. 7c.

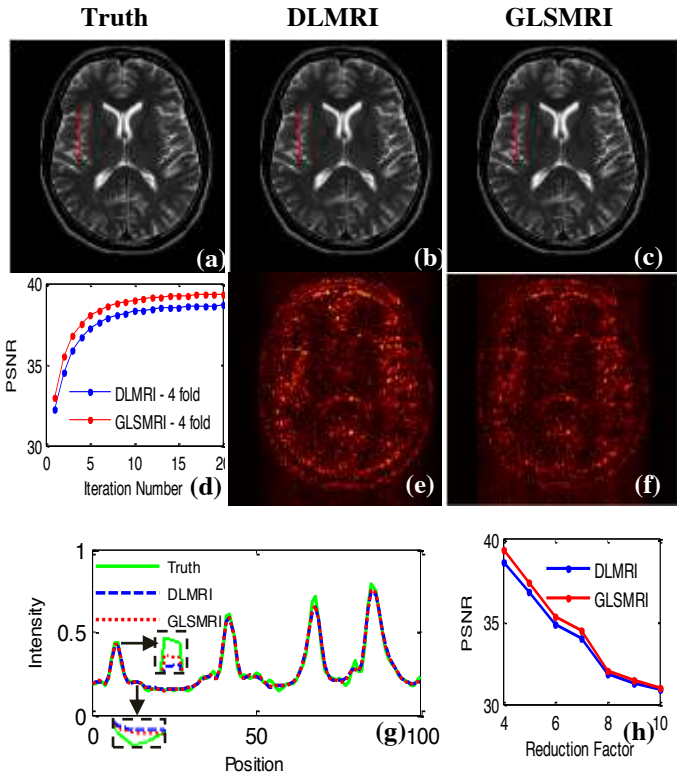

Fig. 5. Comparison of recovered brain using DLMRI and GLSMRI when reduction factor is 4. (a) is the ground truth, (b) and (c) are the output of DLMRI and GLSMRI, respectively. (d) shows the PSNR versus iteration number. (e) and (f) are the error maps, which are multiplied by a factor of 10 for better visualization. (g) shows the curve of intensity for lines marked in (a-c). (h) shows the PSNR versus different reduction factor.

IV. CONCLUSION

We proposed a novel model to reconstruct MR images from under-sampled k-space data by enforcing local and global sparsity constraints to capture details and overall structures of MR images. The model was solved in two steps: local dictionary learning followed by the reconstruction with both local and global sparsity constraints. Simulation results demonstrated that GLSMRI outperformed existing methods, which exploited only local structure or global sparsity structure. The rationale behind selecting several important parameters was also present. Future work will develop robust and efficient patch-level sparse dictionary and use adaptive global sparse dictionary to further improve the reconstruction quality.

V. ACKNOWLEDGE

The work is supported by the Fundamental Research Funds for the Central Universities(CDJZR12090003).

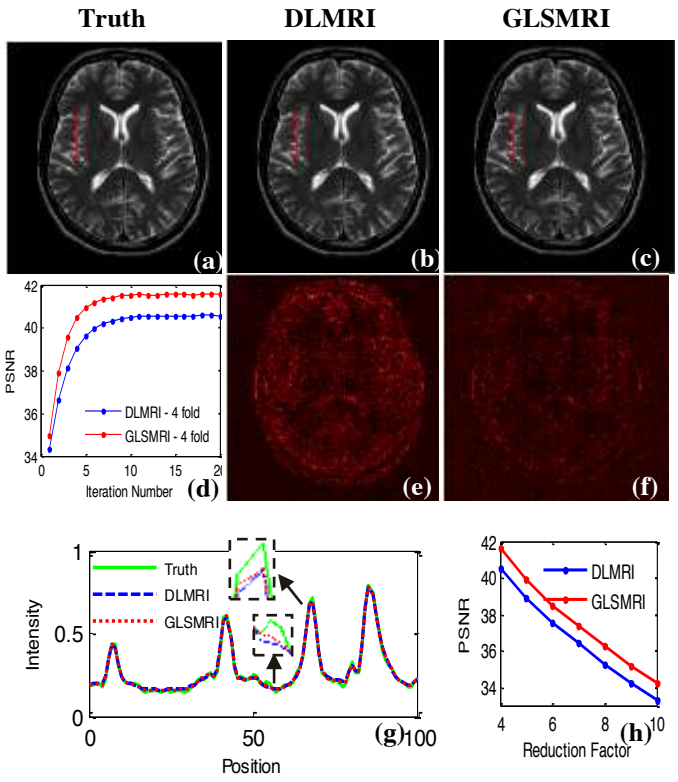

Fig. 6. The same as Figure 5 except that the 2D random sampling pattern was used.

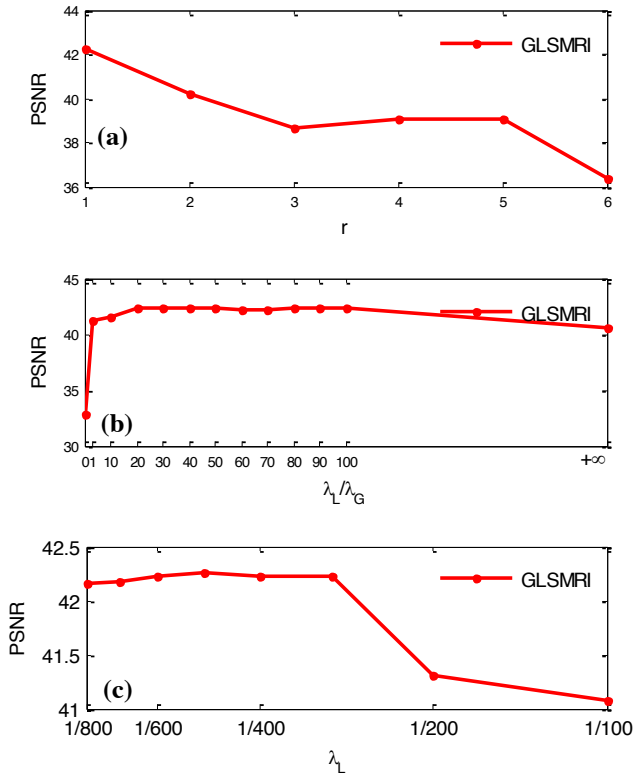

Fig. 7. PSNR versus r(a), λ_L/λ_G(b) and λ_L(c). In (b), when $\lambda_L/\lambda_G = 0$ and $+\infty$, GLMRI degrades to the CS-MRI and DLMRI, respectively.

REFERENCES

[1] Z.-P. Liang, and P. C. Lauterbur, *Principles of magnetic resonance imaging*: *SPIE Optical Engineering Press*, 2000.

[2] D. L. Donoho, "Compressed sensing," *IEEE Trans. Inf. Theory*, vol. 52, no. 4, pp. 1289-1306, 2006.

[3] E. J. Candes, and T. Tao, "Decoding by linear programming," *IEEE Trans. Inf. Theory*, vol. 51, no. 12, pp. 4203-4215, 2005.

[4] E. J. Candès, J. Romberg, and T. Tao, "Robust uncertainty principles: Exact signal reconstruction from highly incomplete frequency information," *IEEE Trans. Inf. Theory*, vol. 52, no. 2, pp.489-509, 2006.

[5] M. Lustig, D. Donoho, and J. M. Pauly, "Sparse MRI: The application of compressed sensing for rapid MR imaging," *Magn.Reson.Med.*, vol. 58, no. 6, pp. 1182-1195, 2007.

[6] E. Candes, L. Demanet, D. Donoho, and L. Ying, "Fast discrete curvelet transforms," *Multiscale.Model.Sim*, vol. 5, no. 3, pp. 861-899, 2006.

[7] M. Hong, Y. Yu, H. Wang, F. Liu, and S. Crozier, "Compressed sensing MRI with singular value decomposition-based sparsity basis," *Phys.med.biol*, vol. 56, no. 19, pp. 6311, 2011.

[8] M. Aharon, M. Elad, and A. Bruckstein "K-SVD - An Algorithm for Designing Overcomplete Dictionaries for Sparse Representation," *IEEE Trans. Signal Process.*, vol. 51, no. 12. pp. 4203-4215, 2006.

[9] J. Yang, J. Wright, T. S. Huang, and Y. Ma, "Image super-resolution via sparse representation," *IEEE Trans.Image Process*, vol. 19, no. 11, pp. 2861-2873, 2010.

[10] M. Aharon, and M. Elad, "Sparse and redundant modeling of image content using an image-signature-dictionary," *SIAM.J.Imaging.Sci*, vol. 1, no. 3, pp. 228-247, 2008.

[11] X. Qu, D. Guo, B. Ning, Y. Hou, Y. Lin, S. Cai, and Z. Chen, "Undersampled MRI reconstruction with patch-based directional wavelets," *Magn.Reson.Imag*, vol. 30, no. 7., pp. 964-977,2012.

[12] Y. Wang, L. Ying, "Compressed Sensing Dynamic Cardiac Cine MRI Using Learned Spatiotemporal Dictionary," *IEEE Trans. Bio-Med Eng*, vol. 61, no. 4, pp. 1109-1120, 2014.

[13] S. Ravishankar and Y. Bresler "MR Image Reconstruction From Highly Undersampled k-Space Data by Dictionary Learning," *IEEE Trans. Med Imag*, vol.30. no. 5, pp. 1028-1041, 2011.

[14] W. Dong, X. Li, Y. Ma, and G. Shi, "Image restoration via Bayesian structured sparse coding," *IEEE Int. Conf. Image Process*, pp. 4018-4022, 2014.

[15] S. Pejoski V. Kafedziski and D. Gleich, "Compressed Sensing MRI Using Discrete Nonseparable Shearlet Transform and FISTA," *IEEE Signal Process. Lett.*, vol. 22, no. 10, pp. 1566-1570, 2015.

[16] R. Venkataramani, and Y. Bresler, "Further results on spectrum blind sampling of 2D signals," *IEEE Int. Conf. Image Process*, vol. 2, pp. 752–756, 1998.

[17] J. Tropp, "Greed is good: Algorithmic results for sparse approximation, I *IEEE Trans. Inf. Theory*, vol. 50, no. 10, pp. 2231-2242,2004.

[18] J. Nocedal, and S. J. Wright, "Conjugate gradient methods," *Numerical Optimization*, pp. 101-134, 2006.

[19] X. Peng, and D. Liang, " MR Image Reconstruction with Convolutional Characteristic Constraint (CoCCo)," *IEEE Signal Process. Lett.*, vol. 22, no. 8, pp. 1184-1188, 2015.

[20] American Radiology Services, 2009 [Online]. Available: http://www3.americanradiology.com/pls/web1/wwimggal.vmg/